3D SIMULATION OF THE MELTING DURING A N ELECTRO-SLAG REMELTING PROCESS

A. Kharicha[(1)], A. Ludwig[(2)], M. Wu[(2)]
[(1)] CD-Laboratory for Multi-Phase Modelling of Metallurgical Processes
[(2)] University of Leoben,
Franz-Joseph Strasse 18. 8700 Leoben, AUSTRIA,
abdellah.kharicha@uni-leoben.at

Keywords: Electroslag, droplet formation, melting, MHD, VOF, Simulation, Joule Heating, electric current, magnetic field

Abstract

The droplet formation during melting of a 400 mm diameter electrode is simulated with a multiphase-MHD approach. The computational model includes a layer of slag and a layer of liquid steel. A VOF approach is used for the interface tracking and a potential formulation is used for the electric and the magnetic field. The Lorentz force and the Joule heating are recalculated at each time step in function of the phase distribution. The first results provided by this model are presented.

Introduction

The Electro-Slag-Remelting (ESR) process is an advanced technology for the production of components of e.g. high quality steels [1-9]. An alternating current (Figure 1) is passed from a conventionally melted and cast solid electrode through a layer of molten slag to the baseplate. Because of the electrical resistivity of the slag, Joule heating is generated and the slag transfers this energy to ingot and mould surfaces and to the melting electrode tip. The molten metal produced in the form of droplets passes through the slag and feeds a liquid pool from where directional solidification takes place. The slag and the ingot are contained in a water cooled copper mould. As also the baseplate is water cooled, a heat flow regime is imposed that gives controlled solidification, and this results in improved structure characteristics of ESR ingots.

This process involves two liquids, a liquid metal and a liquid slag. Each liquid is subject to a phase change due to melting and/or solidification. From a fluid dynamic point of view, the ESR process is clearly a multiphase process, with free interfaces (slag/pool, gas/slag), and with a mixed area (slag and falling steel droplets) [10-15].

Physically, the development of the heat and mass transfer at the slag/droplet interface is important for the final ingot quality, composition and cleanliness. Visual observations of the droplet formation just under the electrode being melted is almost impossible. Due to the presence of high temperatures, opacity of the materials, and the presence of the mould it is not possible to directly observe the behaviour the slag/pool interface. Although usually assumed flat [1-9], a previous work [10] using a Volume of fluid (VOF) model has shown that the interface shape between a layer of slag and steel layer in a cylindrical cavity is highly coupled with the distribution of the electric current. A full scale simulation of the ESR process using a VOF model has shown that the shape of the pool interface is likely to be non flat. Depending on whether a “flat” or “free” interface is assumed, an appreciable difference was found in the prediction of the pool shape and depth [10]. This difference is due to a different magnitude

and distribution of the Joule heat generated.

For fundamental and technical reasons it is important to study how the droplets form and behave in the slag. Usually the effects of the droplets are essentially taken into account in the form of a momentum and energy source applied to slag and pool regions [8]. Nevertheless this approach needs an empirical or semi-empirical radial droplet distribution, and droplet temperatures. The latest is often selected according to the resulting pool shape. However, as the steel/slag density and viscosity ratio are neither very large nor very small, one can expect an important transfer of momentum between the droplets and the slag flow. And, as the electric conductivity of steel is known to be much higher than that of the slag, the distribution of the steel phase within the slag will be a critical parameter to predict the distribution of the electric current density which controls the Lorentz force magnitude. From these physical facts, one can expect in this nonlinear system a slight change in the distribution of the steel droplets in the slag can result in totally different flow behavior.

The present model was recently applied on the melting of a small electrode (35 mm). It was shown that with large surface tension only one faucet forms and larger droplets are released. The fluctuation of the resistance can easily be interpreted as lower picks occur during the release of each primary or secondary droplet. For small surface tension, two to three faucets appear from which smaller droplets depart. In this case the space between the electrode and the liquid pool surface is filled with many small droplets. The continuous release of droplets generates constant electric resistance fluctuations. In this configuration it was not possible to clearly link the resistance signal with a phase distribution in the cavity.

The model is now used to explore the droplet formation during the melting of an industrial scale electrode. During the process the electrode can develop a flat or a parabolic surface, here it is assumed flat. The electric current distribution is dynamically calculated from the transient phase distribution. Then the electromagnetic forces and the Joule heating are recalculated at each time step.

Numerical Model

The calculation domain is a cylinder of 20 cm high and 30 cm radius. The electrode has a radius of 21 cm. The container is filled with the quantity of liquid slag (10 cm high) and liquid steel (10 cm high). The total number of volume elements is 13.8 million cells. Material properties of steel and slag are assumed to be constant. The electrode supplies a total DC current of I_0 = 13 000 Amperes.

The interface between the two phases is tracked with the geometric reconstruction VOF technique. A single set of momentum equations is shared by the fluids, and the volume fraction of each of the fluids in each computational cell is tracked throughout the domain. According to the local value of the volume fraction *f*, appropriate properties and variables are assigned to each control volume within the domain. In a two phase system the properties appearing in the momentum equation are determined by the presence of the component phase in each control volume. The local values of a physical property Θ (such as density, viscosity, electric conductivity) are interpolated by the following formula $\Theta = \Theta_1 f_1 + \Theta_2 f_2$, where the subscripts 1,2 indicate the corresponding phase. The value of the surface tension is chosen to be equal to 0.1 or 1N/m. Depending on the dynamic of the interfaces, the typical calculation time step lies in the range of 10^{-3}-10^{-5} second.

Fluid flow: The motion of the slag and liquid steel is computed with the buoyant Navier-

Stokes equations. The effect of the turbulence is estimated with a Smagorinsky LES model. The no-slip condition is applied at the lateral walls. The electrode and the bottom surface are modelled as velocity inlets with a fixed velocity (0.14 mm/s at the electrode) corresponding to a melt rate of about 500 kg/hour.

Electromagnetics: The potential equation is computed from the equation of the conservation of the electric current:

$$\nabla \cdot \vec{j} = \vec{\nabla}(-\sigma \vec{\nabla} V) = 0\,, \tag{1}$$

where V is the electric potential. A flux condition is applied at the bottom surface, while a constant electric potential is applied at the electrode. No current is allowed to enter the mould. The magnetic field is then extracted by solving the magnetic vector potential equation. The computed electromagnetic field is dynamically adjusted from the space distribution of the electric conductivity, which is in turn a function of the predicted phase distribution. The Lorentz force acting on both slag and steel is defined by:

$$\vec{F}_L = \mu_0 \, \vec{j} \times \vec{B}\,. \tag{2}$$

Heat transfer: The energy equation is solved in the fluid domain. The Joule heating is taken as a source term in the energy equation:

$$Q(t) = \frac{j^2(\vec{x},t)}{\sigma(\vec{x},t)} \tag{3}$$

The temperature at the electrode/slag contact surface is fixed at the alloy liquidus temperature. The P1 radiation model is used to compute the radiation in the slag media. At the mould and at the bottom boundary, the temperature is fixed at the slag liquidus temperature. The radiative emissivity of the slag surface is taken equal to 0.8.

Resistance swing: The electric resistance can be calculated at each time from the total Joule heating generated in the domain:

$$Res(t) = \frac{1}{I_0^2} \int \frac{j^2(\vec{x},t)}{\sigma(\vec{x},t)} d\vec{x}^3 \tag{4}$$

The deviation from the average resistance is defined by:

$$\delta Res(t) = (Res(t) - \frac{1}{2T} \int_{-T}^{T} Res(t)dt) / Res(t)\,, \tag{5}$$

where T is an averaging time large enough to include several droplet departures.

Results and Discussion

To show the results we choose to plot the fields over the surface of a constant slag fraction ($f_1 = 0.5$) and over the x = 0 plane (Figures 2-5). The iso-volume fraction represents two surfaces, first is the slag/pool interface, and the second is the surface enveloping the thin liquid film that develops just under the electrode. It is then clear that the iso-volume fraction surface changes constantly its shape with time, while the iso-x plane can be represented as a vertical curtain that hides what happens behind it. Between these two surfaces, the iso-volume fraction visualizes also the falling droplets.

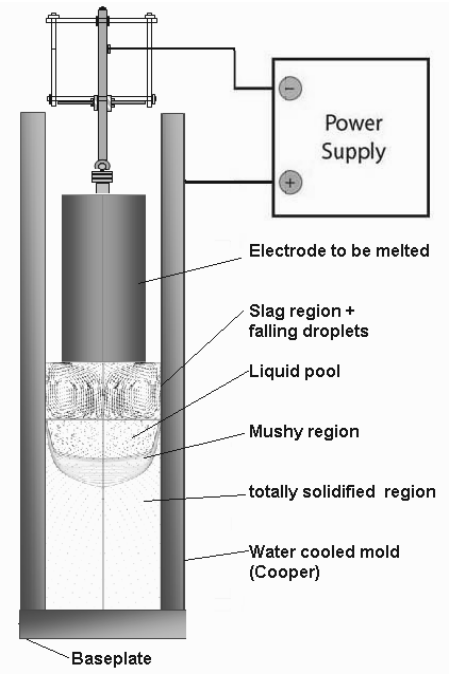

Figure 1: Schematic view of the ESR system.

Figure 2 represents the evolution the electric current density during the formation and the departure of several droplets. To minimize the electric resistance, the electric current chooses in priority to travel through the liquid metal. The typical liquid film thickness was found to be around 1-1.5mm.The formation of a droplet starts by the thickening of the liquid film (5-7 mm) in a form of a bag. In figure 2 a we can observe almost 20 positions from where the droplets can possibly depart. When the thickness of the liquid film bag exceeds 13 mm an elongated faucet forms. The electric current density increases strongly during the faucet formation. But when the departure of the first droplet occurs a slag gap forms between the drop and the remaining faucet, leading to a decrease in the current density. The electric current density decreases to lower values during the departure of smaller droplets (satellite droplets). The equivalent droplets diameter was found to be 10-15 mm for the largest, and 1-4 mm for the satellite droplets. During the fall, the large droplets flatten and develop a lentil or a crescent shape. The depressions (with low electric current density) created by the impacts on the slag/pool interface can easily be observed in figure 2 c-f).

Classically from 2D single phase calculations, the position of maximum Joule heating release (Q) is situated at the vicinity of the electrode periphery. This is still observed in figure 3, however the volume that surrounds the faucets and the droplets witnesses also strong fluctuation in power generation. Outside this region, i.e. near the mould under the exposed slag surface, the flow shows an almost axisymmetric and steady pattern. The non flat liquid film generates additional heat release regions (under the liquid metal bags). During the droplet formation, the magnitude of Q reaches even similar values than those observed in the periphery of the electrode ($Q \sim 10^9$).

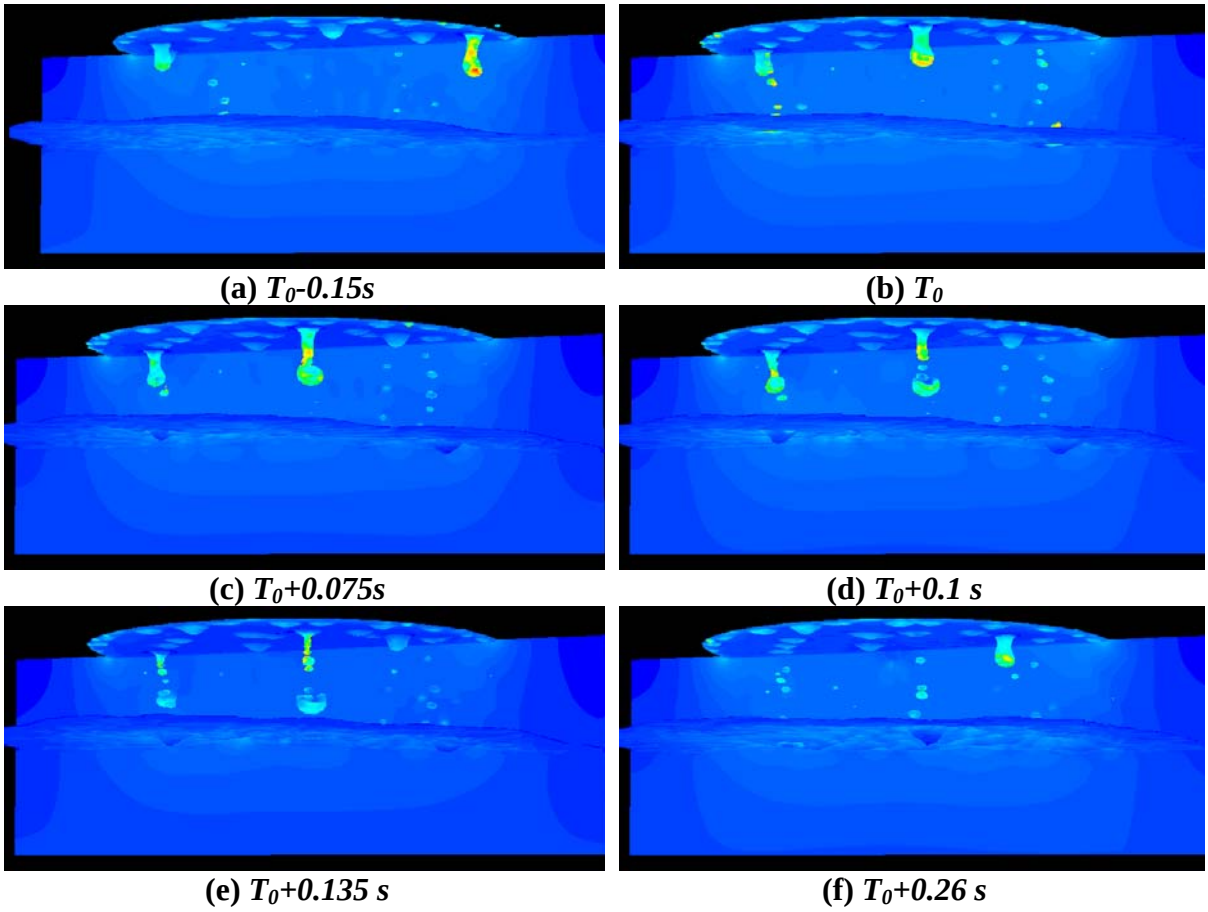

Figure 2: Electric current density [4.10^4 - 2.10^6 A/m2]

The characteristic time between the departure and the impact of a droplet is of about 0.25-1 second. Compared to this time the temperature and the main flow field (figure 4-5) are much more stable. The temperature distribution shows that the hottest region is localised in the slag between the electrode and the pool interface. Previous 2D approaches [1-9] have predicted a maximum localised between the exposed slag surface and in the vicinity of the mould. In those publications the droplets were only supposed to transfer a part of the slag heat to the liquid pool, generating a negative heat source in the area localised under the electrode. In addition these models neglected the effect of the droplets on the electric current distribution and on the Joule heat generation.

The velocity magnitude reaches a maximum of 0.65 m/s, however this speed correspond to the maximum speed of the falling droplets. The slag region affected by the droplets trajectory is strongly turbulent, from the 5 pictures given in figure 5 it is not possible to draw a main flow pattern. This is a strong indication that a strong momentum exchange occurs between the slag and the metallic droplets. Outside the droplets falling region the main flow velocity does not exceed 0.18 m/s, but surprisingly the flow in the liquid pool was found to be as strong as in the liquid slag.

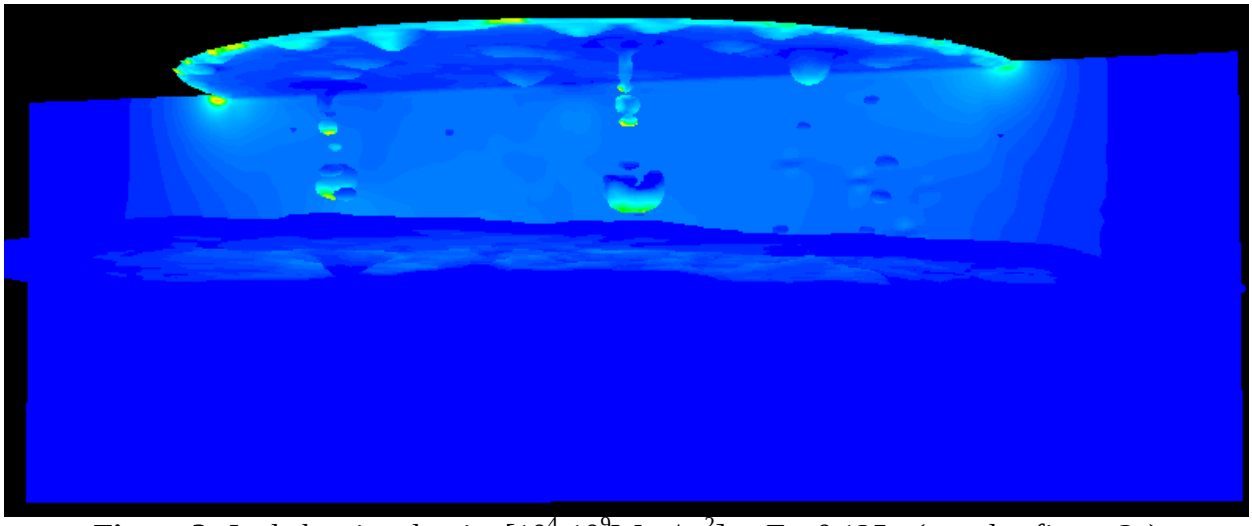

Figure 3: Joule heating density [10^4-10^9Watt/m^2] at T_0+*0.135 s* (see also figure 2e)

The movement of the liquid-pool interface is clearly observable in figures 4-5. Its movements has a strong non axisymetric behaviour, resulting from MHD actions such those observed in aluminium reduction cells. However the falling droplets might also influence the dynamic of the interface, through their momentum impacts, but also by their influence on the current distribution within the slag layer. The redistribution of the liquid metal within the liquid pool induces strong flow in azimuthal direction. These results question the validity of the axis-symmetric hypothesis for the 2D calculations.

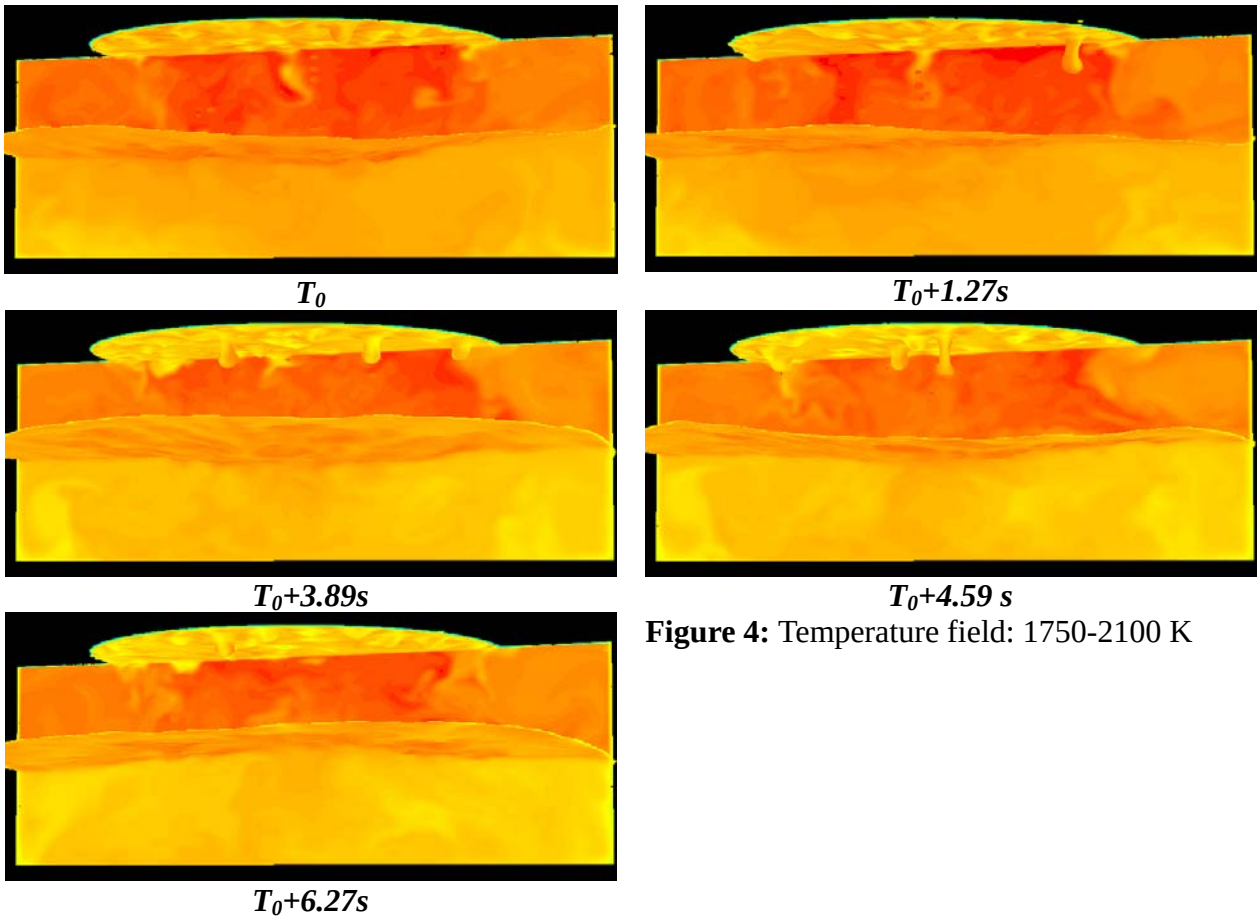

Figure 4: Temperature field: 1750-2100 K

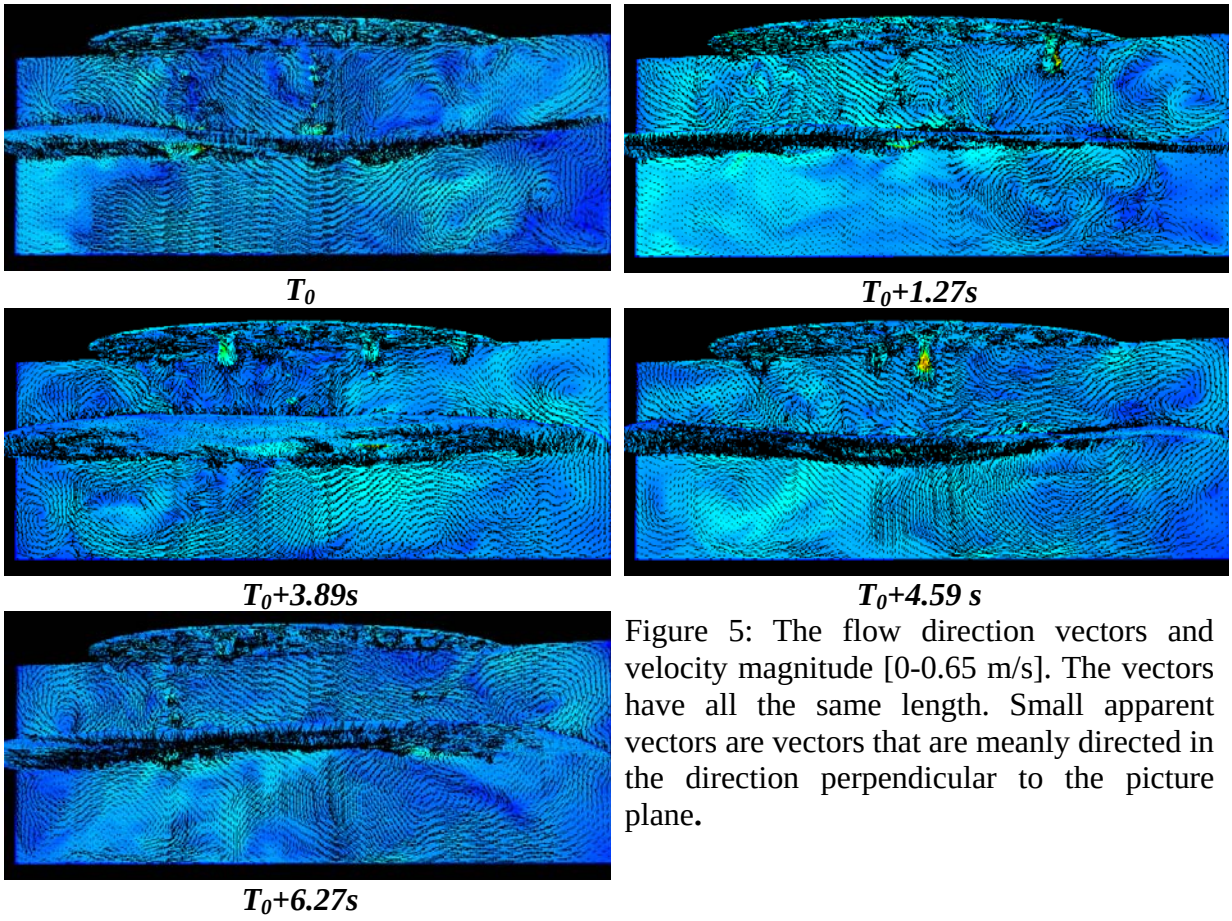

Figure 5: The flow direction vectors and velocity magnitude [0-0.65 m/s]. The vectors have all the same length. Small apparent vectors are vectors that are meanly directed in the direction perpendicular to the picture plane**.**

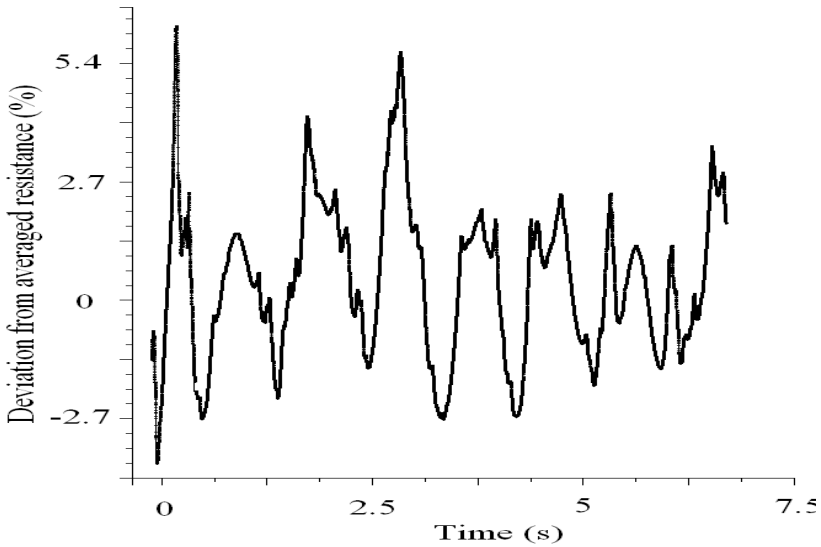

Figure 6: Fluctuation of the resistance during melting.

The electric resistance fluctuates around its mean value depending on the metal distribution in the calculation domain (figure 6). The fluctuations can reach 5% at some points, but in average it is lower than 1.5 %. The lowest resistance picks correspond to situations where a long faucet is present, and the highest correspond to situations with a minimum of droplets between the electrode and the interface. The movement of the interface can also affects the resistance path by decreasing at some position the distance between the electrode and the liquid pool. It can

be noticed that the maximum and the minimum picks follows a tendency, they can be enveloped or modulated by waves of smaller frequency. We think that the movement of the interface acts as a modulator on the amplitude of the fast fluctuations generated by the droplets fall.

Conclusions

A 3D VOF model was coupled with a Magnetohydrodynamic model to simulate the droplet formation during melting of electrode. The model can predict the electric and magnetic field distribution in function of the metallic distribution in the low electric conductivity slag. The model was applied to the melting of an industrial scale mall electrode assuming a constant melting rate and a constant imposed DC electric current intensity.

The results can be summarized in five points:

1) The droplets formation, departure, and movement in the slag disturb the distribution of the electric current density. This induces an additional Joule heating generation just under the electrode. Thus, the area between the electrode and the pool interface is the warmest region.
2) The droplets have diameters of about 1-15 mm. During their fall they generate strong turbulences in the slag flow.
3) Due to MHD forces and to the droplets impacts, the liquid pool interface moves with a non axis-symmetric pattern. The amplitude of the movements reaches 5 cm.
4) Both the interface and droplets contributes to the existence of a non axis-symmetric mean flow.

In this work a DC current was assumed, however most of the conclusions given here are believed to be still valid when an AC current is applied.

References

[1] Mitchell A., Joshi S., Cameron J., *Metall. Trans.*, vol. 2B, 1971, p. 561.
[2] Hoyle G., *Electroslag Processes, Principles and Practice*, Elservier Sci. Ltd (ISBN 0-85334-164-8),1983.
[3] Zak E.D., *Proc. Vacuum Metall. Conf.*, Pittsburgh, 1977.
[4] Choudhary M., Szekely J., *Metall. Trans. B*, vol. 11B, 1980, p. 439.
[5] Dilawari A.H., Szekely J., *Metall. Trans. B*, vol. 8B, 1977, p. 227.
[6] Choudhary M., Szekely J., *Ironmaking and Steelmaking*, vol. 5, 1981, p. 225.
[7] Jardy A., Ablitzer D., Wadier J. F., *Metall. Trans.*, vol. 22B, 1991, p. 111.
[8] Hernandez-Morales B., Mitchell A., *Ironmaking and Steelmaking*, vol. 26, 1999, p. 423.
[9] Kelkar K.M., Mok J., Patankar S.V., Mitchell A., *Phys. IV France*, vol. 120, 2004, p. 421.
[10] Kharicha A., Schützenhöfer W., Ludwig A., Tanzer R., Wu., *Steel Res. Int.*, vol.79 (8), 2008, p. 632-636.
[11] Kharicha A., Schützenhöfer W., Ludwig A., Tanzer R.. Wu M., *Int. J. Cast Metals Res.*, vol. 22, 2009, p. 155-159.
[12] Kharicha A., Schützenhöfer W., Ludwig A., Tanzer R., Wu M., *2nd Int. Conf. Simul. Model. Metallurgical Processes in Steelmaking (STEELSIM 2007)*, Graz, Austria, Sept. 12-14, 2007, ed. Ludwig A., Knittelfeld: Gutenberghaus Druck GmbH, p. 105-110
[13] Kharicha A., Mackenbrock A., Ludwig A., Schützenhöfer W., Maronnier V., Wu M., Köser O., *Int. Sympo. Liquid metal Processing and casting (ICASP 2007)*, Sept. 2-5, 2007, Nancy, France, eds. Lee P.D., Mitchell A., Bellot J.P., Jardy A., p. 107-113.
[14] Kharicha A., Ludwig A., Wu., *Mater. Sci. Eng. A*, vol. 413.414, 2005, p. 129-134.
[15] Kharicha A., Ludwig A., Tanzer R., Schützenhöfer W., *Mater. Sci. Forum*, vol. 649, 2010, p. 229-236.